ORIGINAL ARTICLE

Evaluating the Prediction of Brain Maturity From Functional Connectivity After Motion Artifact Denoising

Ashley N. Nielsen[1], Deanna J. Greene[2,3], Caterina Gratton[1], Nico U.F. Dosenbach[1,4], Steven E. Petersen[1,3,4,5] and Bradley L. Schlaggar[1,2,3,4,6]

[1]Department of Neurology, Washington University School of Medicine, St. Louis, MO 63110, USA, [2]Department of Psychiatry, Washington University School of Medicine, St. Louis, MO 63110, USA, [3]Department of Radiology, Washington University School of Medicine, St. Louis, MO 63110, USA, [4]Department of Pediatrics, Washington University School of Medicine, St. Louis, MO 63110, USA, [5]Department of Psychology, Washington University in St. Louis, St. Louis, MO 63130, USA and [6]Department of Neuroscience, Washington University School of Medicine, St. Louis, MO 63110, USA

Address correspondence to Ashley N. Nielsen, East Building Neuroimaging Laboratories, 4525 Scott Ave, Suite 2220, St. Louis, MO 63110, USA. Email: ashley.nielsen@wustl.edu

Abstract

The ability to make individual-level predictions from neuroanatomy has the potential to be particularly useful in child development. Previously, resting-state functional connectivity (RSFC) MRI has been used to successfully predict maturity and diagnosis of typically and atypically developing individuals. Unfortunately, submillimeter head motion in the scanner produces systematic, distance-dependent differences in RSFC and may contaminate, and potentially facilitate, these predictions. Here, we evaluated individual age prediction with RSFC after stringent motion denoising. Using multivariate machine learning, we found that 57% of the variance in individual RSFC after motion artifact denoising was explained by age, while 4% was explained by residual effects of head motion. When RSFC data were not adequately denoised, 50% of the variance was explained by motion. Reducing motion-related artifact also revealed that prediction did not depend upon characteristics of functional connections previously hypothesized to mediate development (e.g., connection distance). Instead, successful age prediction relied upon sampling functional connections across multiple functional systems with strong, reliable RSFC within an individual. Our results demonstrate that RSFC across the brain is sufficiently robust to make individual-level predictions of maturity in typical development, and hence, may have clinical utility for the diagnosis and prognosis of individuals with atypical developmental trajectories.

Key words: development, fMRI, functional connectivity, machine learning

Introduction

Individual-level prediction about brain maturity has the potential to be useful for the assessment of developmental progress. The ability to identify an individual with an atypical developmental trajectory might facilitate more accurate diagnoses and prognoses of developmental disorders and lead to earlier and individualized treatment (Emerson et al. 2017; Hazlett et al. 2017). Clinically useful neurobiological measurements should be sufficiently robust to make an accurate prediction of the maturity of typically developing individuals and be closely related to the dysfunction in developmental disorders. Multivariate descriptions of these measurements, based on patterns of information, may be

best equipped to make such robust and accurate predictions about an individual child (Bray et al. 2009; Jimura and Poldrack 2012; Sundermann et al. 2014). Measurements of functional connectivity may be more closely linked to behavior/cognition and more likely disrupted in developmental disorders. Resting-state functional connectivity (RSFC) MRI, the temporal correlation between spontaneous fluctuations in blood oxygen level-dependent signals across the brain (Biswal et al. 1995), has been proposed to reflect the statistical history of co-activation across an individual's lifespan (Fox and Raichle 2007; Dosenbach et al. 2008). In addition, RSFC is thought to be disrupted in individuals with an atypical developmental trajectory (Fox and Greicius 2010). Whether or not differences in functionally relevant neurobiology measured with RSFC carry multivariate information germane to make predictions about the health and maturity of an individual child is an important question.

Previously, Dosenbach and colleagues (2010) demonstrated successful prediction of the maturity of individuals based on RSFC using multivariate machine learning (Dosenbach et al. 2010). Using a set of features (i.e., functional connections), they created a multivariate model relating age and RSFC in a training dataset and used this model to successfully predict the age of test individuals. Since then, others have also used machine learning to show that RSFC can make predictions about age (Supekar et al. 2009; Meier et al. 2012; Vergun et al. 2013) as well as various other qualities of individuals, including sex (Casanova et al. 2012) and IQ (Santarnecchi et al. 2014). Additionally, multivariate machine learning approaches have shown that there is information in RSFC to classify healthy individuals from clinical populations including ADHD (Liang et al. 2012), schizophrenia (Fan et al. 2011; Bassett et al. 2012; Du et al. 2012), mild cognitive impairment/Alzheimer's disease (Koch et al. 2012; Wee et al. 2012), major depressive disorder (Craddock et al. 2009), and autism (Nielsen et al. 2013; Chen et al. 2016). Taken together, these results suggest that differences in RSFC carry information important to representing and making predictions about the individual.

Unfortunately, the success of many previous RSFC studies using machine learning to make predictions about individuals may be contaminated by (even submillimeter level) subject head motion in the scanner. Small amplitude movements in the scanner have been shown to have systematic effects on observed resting-state correlations; this motion-related artifact is distance-dependent, such that correlations are increased for short-range connections and decreased for long-range connections, with specific sets of functional connections being more affected than others (Power et al. 2012, 2014; Van Dijk et al. 2012; Satterthwaite, Elliott, et al. 2013; Ciric et al. 2017). Motion-related artifact is problematic for machine learning approaches because head motion is often correlated to the characteristics being predicted (e.g., age, disease status, IQ) (Siegel et al. 2016). Fortunately, we and others have developed methods to reduce the adverse effects of motion-related artifact and other sources of physiological noise on functional MRI data (Power et al. 2014; Ciric et al. 2017). With these denoising approaches as well as approaches that pre-emptively reduce head movements (Dosenbach et al. 2017; Greene et al. 2018), many have worked to validate previous machine learning results using RSFC after attempting to correct for individual differences in head motion (Fair et al. 2013; Greene et al. 2014; Pruett et al. 2015; Greene, Church, et al. 2016; Emerson et al. 2017). Specifically, there is growing evidence that after reducing artifactual differences in RSFC related to movement, by including signal processing and strict subject matching/selection (Fair et al. 2013; Satterthwaite, Wolf, et al. 2013; Greene, Black, et al. 2016), RSFC can still be used to successfully predict an individual's age.

The present work has 2 major aims related to evaluating the prediction of age from RSFC after motion denoising. First, we aimed to evaluate whether or not there are lingering multivariate effects of head motion on resting-state correlations that contribute to age prediction. We tested whether patterns of RSFC can be used to predict an individual's age and an individual's in-scanner head movement using machine learning before and after reducing motion-related artifact. Ensuring that head motion cannot be predicted from RSFC after motion denoising using machine learning is important for assessing the viability of RSFC as an indicator of developmental progress rather than confounding transient characteristics of individuals. Second, we were interested in evaluating the specific functional connections that facilitate age prediction after reducing motion-related artifact. Previously, Dosenbach et al. (2010) identified a set of functional connections thought to best predict age using a fairly straightforward data-driven, feature selection scheme (i.e., ranking the functional connections most correlated with age). Of these top ranked functional connections, many were short-range and long-range connections, in accordance with the the "local-to-distributed" theory of RSFC development (short-range became weaker and long-range became stronger with maturity) (Fair et al. 2009; Supekar et al. 2009). However, developmental differences in head motion produce differences in RSFC that reproduce this pattern (i.e., with less subject head motion, short-range functional connections become weaker while long-range functional connections become stronger). Thus, we aimed to identify the functional connections that best predict age and test the "local-to-distributed" hypothesis of RSFC development after reducing motion-related artifact. More recently, investigators have used feature selection to experimentally manipulate the information available for prediction and compare the resulting predictive performance. Whether prediction with RSFC depends upon a hypothesized, organizing principle (e.g., functional systems (Du et al. 2012; Koch et al. 2012; Uddin et al. 2013; Greene, Church, et al. 2016), RSFC strength (Bassett et al. 2012; Santarnecchi et al. 2014)), can be assessed by selecting and testing a set of features with specific properties. Therefore, we also sought to determine whether other organizing principles (e.g., functional systems, RSFC strength) facilitate age prediction with hypothesis-driven feature selection.

Materials and Methods

Participants

A group of 122 healthy children and adults (ages 7–31 years old, 66 males) were selected from an extant database of participants ($n = 487$, ages 6–35 years old, 206 males) on the basis of having at least 120 data frames (~5 min) of usable resting-state fMRI data (as defined below). Participants were recruited from the Washington University campus and the surrounding community. All participants were native English speakers, right-handed, and reported no history of neurological or psychiatric disease or a current prescription of psychotropic medications (parental report for child participants). All adult participants, and a parent or guardian for each child participant, gave informed consent, and all children assented to data collection. All participants were compensated for their participation. The Washington University Human Research Protection Office approved all studies.

Image Processing

Image Acquisition
Data were collected on a Siemens 3 T MAGNETOM Trio scanner with a Siemens 12-channel Head Matrix Coil. To help stabilize

head position, each subject was fitted with a thermoplastic mask fastened to holders on the head coil. A T1-weighted sagittal MP-RAGE structural image (slice time echo, 3.06 ms; TR 2.4 s; inversion time, 1 s; flip angle, 8°; 127 slices; $1 \times 1 \times 1\,mm^3$ voxels) in the same anatomical plane as the BOLD images were obtained to improve alignment to an atlas. Functional images were acquired using a BOLD contrast-sensitive echo planar sequence (TE, 27 ms; flip angle, 90°, in-plane resolution, $4 \times 4\,mm^2$; volume TR 2.5 s). Whole-brain coverage was obtained with 32 contiguous interleaved 4 mm axial slices. Steady-state magnetization was assumed after 4 volumes. The total number of resting-state functional volumes acquired ranged from 184 to 780. The length of each resting-state run ranged from 5 to 30 min.

During the resting-state scans, participants viewed a centrally presented white crosshair (subtending <1° visual angle) on a black background. Participants were instructed to relax, "keep an eye on the plus sign", and hold as still as possible.

Image Analysis

Functional images from each participant were preprocessed to reduce artifacts (Shulman et al. 2010). These steps included: 1) temporal sinc interpolation of all slices to the temporal midpoint of the first slice, accounting for differences in the acquisition time of each individual slice, 2) correction for head movement within and across runs, and 3) intensity normalization of the functional data was computed for each individual via the MP-RAGE T1-weighted scans. Each run was then resampled in atlas space on an isotropic 3 mm grid combining movement correction and atlas transformation in a single interpolation. The target atlas was created from thirteen children (7–9 years old) and twelve adults (12–30 years old) using validated methods (Black et al. 2004). The atlas was constructed to conform to the Talairach atlas space.

Several additional preprocessing steps were applied to reduce spurious variance unlikely to reflect neuronal activity (Fox et al. 2009). These RSFC preprocessing steps included: 1) demeaning and detrending each run, 2) multiple regression of nuisance variables, 3) frame censoring (discussed below) and interpolation of data within each run, 4) temporal band-pass filtering ($0.009\,Hz < f < 0.08\,Hz$), and 5) spatial smoothing (6 mm full width at half maximum). Nuisance variables included motion regressors (e.g., original motion estimates, motion derivatives, and Volterra expansion of motion estimates), an average of the signal across the whole brain (global signal), individualized ventricular and white matter signals, and the derivatives of these signals.

Reducing Head Motion-Related Artifact

We applied a procedure determined and validated to best reduce artifacts related to head motion (Power et al. 2014; Ciric et al. 2017). With this approach to reducing motion-related artifact, we can re-evaluate whether patterns of RSFC can predict an individual's age, but not age-related head movement.

Specifically, frame-by-frame head displacement (FD) was calculated from preprocessing realignment estimates, and frames with FD > 0.2 mm were removed. An FD threshold of 0.2 mm was chosen because it best reduced the distance-dependence related to individual differences in head motion (estimated with mean FD and 6 motion parameters) in this developmental dataset, as assessed using procedures from Power et al. (2012) and Ciric et al. (2017) (see Supplemental Material A). Data were considered usable only in contiguous sets of at least 3 frames with FD < 0.2 and a minimum of 50 frames within a functional run. "Bad" frames were censored from the continuous, processed resting-state time series before computing resting-state correlations. Notably, the global signal was included as a nuisance regressor (mentioned above) in order to further reduce global, motion-related spikes in BOLD data (Power et al. 2014; Ciric et al. 2017). To avoid motion-related differences in the amount of data used to calculate resting-state correlations across participants, 120 randomly selected "good" frames of usable data (i.e., frames surviving motion censoring) from each participant were included in further analysis.

To quantify how motion censoring and global signal regression (GSR) affect multivariate prediction with RSFC, we performed additional analyses with 1) no motion denoising (no GSR + no frame censoring) and 2) partial motion denoising (GSR + no frame censoring and no GSR + frame censoring).

RSFC Network Construction

For each participant, resting-state time courses were extracted from a set of 264 previously defined regions of interest (ROIs) covering much of the brain shown in Figure 1A (Power et al. 2011). A weighted correlation matrix representing an individual's RSFC was constructed by calculating the correlation between time-courses from each pair of ROIs and normalizing these values with a Fisher transform. The group average correlation matrix for this developmental dataset is shown in Figure 1B. The RSFC between these 264 ROIs reveals the organization of separable functional systems (e.g., default-mode, frontoparietal, visual) in both children and adults (Power et al. 2011; Yeo et al. 2011).

Support Vector Regression

Support vector machine (SVM) learning was used to determine how well an individual's chronological age can be predicted from that individual's pattern of RSFC. We used the Spider Machine Learning Toolbox implemented in Matlab for SVM training and testing. Commonly, SVM is used to test whether patterns of RSFC can classify an individual as a part of a group, a binary label. This approach can be extended to the prediction of continuous labels (e.g., chronological age) using support vector machine regression (SVR). Briefly, SVR extracts the multivariate relationship between features (here, functional connections) and labels (here, age) from a training set of individuals with known labels. Further description of the parameters employed from multivariate machine learning is provided in Supplemental Material B.

We used a 10-fold cross-validation (10-fold CV) procedure in which 10% of the participants were removed from the training set, a multivariate model was generated from the remaining participants (90% of the participants), and the left out participants were tested on the SVR-derived model. For each fold of CV, a different set of 10% of participants were removed from the training set and tested on the SVR-derived model. We tested the robustness of the SVR-derived models with 3 iterations of 10-fold CV (2 iterations are shown in Supplemental Material E, Fig. S3). We also used a leave-one-out cross-validation (LOOCV) procedure for consistency with Dosenbach et al. 2010 and to test the robustness of the results across cross-validation techniques. We found minimal differences between 10-fold CV and LOOCV (LOOCV results are provided in Supplemental Material F, Figure S4).

The extent to which this derived model explains the label-related variance can be determined by applying the SVR-derived model to the features from a test individual outside of the training set and comparing the test individual's SVR
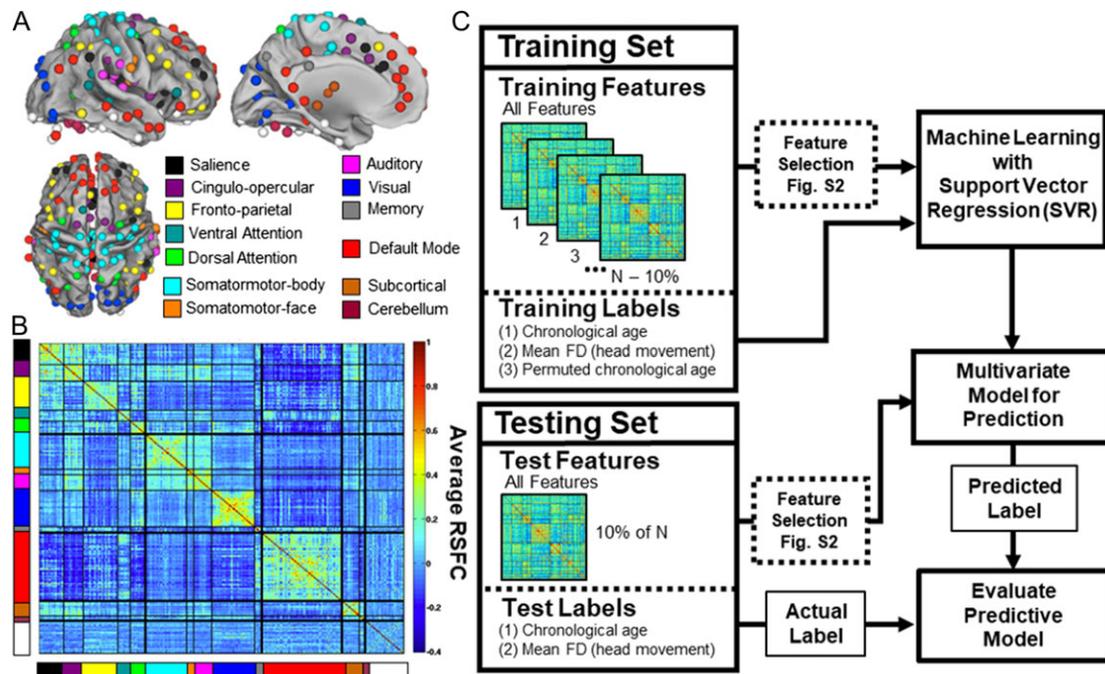
Figure 1. Overview of support vector machine learning with RSFC. (A) Regions of interest (*n* = 264), defined in Power et al. (2011), used to create RSFC correlation matrices. Resting-state time courses were extracted from each of these regions. (B) Average resting-state functional connectivity across all participants. Correlations between the resting-state time courses of all pairs of regions from (A) were sorted according to functional system and average across all subjects included in this analysis. (C) Support vector regression was used to determine a multivariate model for prediction in a training set and this predictive model was evaluated by comparing the predicted labels and actual labels of individuals in a separate testing set. Different training labels (e.g., age, mean FD) were used to create multivariate models to predict different characteristics of individuals using RSFC. In some cases, feature selection was applied before training and testing (for specifics, see Fig. S2).

predicted label and actual label. Previously, Dosenbach et al. 2010 compared several models in order to best fit the relationship between the predicted ages and actual ages of individuals. Here, we chose to use a simple, linear model in order to compare predictive performance across a variety of SVR-models built to predict different labels and built from different sets of features. A schematic of the training and testing in SVR is shown in Figure 1C.

Predicting an Individual's Age
We used SVR to predict the age of each participant and determine whether there are age-related differences in individual patterns of RSFC. Using 10-fold CV, participants were removed from the training set and a multivariate model describing the relationship between RSFC and age was generated in the remaining participants. The left-out participants were then tested on this SVR-derived model yielding a SVR-predicted age for each participant. This process was repeated, resulting in a predicted age for every subject. Predicted ages were then compared with the true ages for each participant.

In order to identify the noise floor for prediction, we permuted the age labels of each participant in the training set. We used the same machine learning approach to assess how well SVR can use patterns of RSFC with fabricated relationships with age. We used the same 10-fold CV procedure as described above, but trained on the permuted age labels rather than the actual ages.

Predicting an Individual's Head Motion
Because of the issue of subject motion contaminating developmental neuroimaging data (Power et al. 2012; Satterthwaite,

Elliott, et al. 2013), we took a conservative approach to identifying potentially lurking, motion-related differences in RSFC that might spuriously enhance our ability to predict age. We used the same machine learning approach to determine whether patterns of RSFC could predict measurements of an individual participant's head movement. Using 10-fold CV, a multivariate model describing the relationship between RSFC and head motion—measured as mean FD—was generated and the left out participants were then tested on this SVR-derived model. Specifically, mean FD was calculated on the preframe censored data, thus quantifying the amount of movement during the entirety of the runs included for each participant. This process was repeated to predict each individual's mean FD. The predicted mean FD was then compared with the true mean FD for that participant. Similar analyses were also conducted using mean FD calculated on the postframe censored data, which measures the residual head motion after denoising (Supplemental Material C). To assess the impact of motion denoising on RSFC, multivariate models describing the relationship between mean FD and RSFC that did not undergo motion denoising (GSR + frame censoring) were also generated and tested.

Prediction Across Feature Numbers
We aimed to explore how the number of features used to create the multivariate model affects the ability to predict age and head motion. We randomly selected functional connections from the entire correlation matrix, sampling between 100 and 19 000 features (out of the possible 34 716) in logarithmic increments. A total of 25 random feature sets were generated for each of the 45 feature numbers sampled. With these feature sets, we tested how well SVR can identify patterns of RSFC

related to age, head motion, and permuted age labels in order to make predictions about individuals. Using 10-fold CV, a multivariate model describing the relationship between these labels and RSFC in randomly selected functional connections was generated and the left out participants were then tested on this SVR-derived model.

Feature Selection

Feature selection is a standard approach in the field of machine learning whose objective is to remove irrelevant features to reduce computational burden, avoid overfitting, and potentially improve predictive performance (Guyon and Elisseeff 2003). Many investigators have interrogated the features derived from feature selection—in the case of RSFC, functional connections—facilitating prediction. The identified, reduced set of functional connections has often been interpreted as meaningful to the mechanism underlying the predicted characteristic (e.g., maturation, disease). We used feature selection to investigate which functional connections carry information useful for age prediction using both data-driven (features defined in a training set) and hypothesis-driven (features defined a priori) approaches. Before interpreting these identified features as meaningful to the mechanism(s) underlying typical development, we compared the performance of selected features to a null model built from a matched set of randomly selected features. Supplemental Material Figure S2 summarizes the types of feature selection used for age prediction.

Data-Driven Feature Selection

Univariate feature ranking and selection in a training set. As a simple approach to identify the best features to predict an individual's age, we ranked and selected features according to the univariate correlation between each functional connection and age across subjects, as in Dosenbach et al. (2010). For each fold of CV, features were ranked according to the strength of the correlation between RSFC and age in the remaining subjects in the training set (note: this approach is different than features ranked according to the RSFC strength within an individual; see RSFC Strength, below). We sampled between 100 and 19 000 top ranked features in logarithmic increments, generated a multivariate model describing the relationship between age and RSFC in these features, and tested the left out participants on the SVR-derived models.

Matched feature set and null model comparison. We evaluated whether these functional connections with strong age relationships were the most useful for multivariate age prediction by contrasting them with a matched set of randomly selected features (see Prediction Across Feature Numbers). We generated a multivariate model describing the relationship between age and RSFC in these randomly selected features, tested the left out participants on the SVR-derived models, and compared the performance of top ranked features with randomly selected features.

Hypothesis-Driven Feature Selection

Beyond identifying a set of features most related to age as described above, we were also interested in experimentally manipulating the information available for age prediction. We aimed to test whether development relies upon organizing principles of RSFC such as connection distance, the definition of functional systems, or the strength of correlations.

Connection distance. Previously, Dosenbach et al. (2010) described evidence that connection distance might underlie the usefulness of functional connections for age prediction. To compare how functional connections of different connection distance contribute to age prediction, we divided the resting-state correlations into 10 separate windows (3471 functional connections per window) based on the distance of the connections in template Talairach space (computed via Euclidean volumetric distance among group ROIs). Using 10-fold CV, a multivariate model describing the relationship between age and the RSFC in these functional connections of a particular length (e.g., short-range, long-range) was determined and the left out participants were then tested on this SVR-derived model.

Matched feature set and null model comparison. We compared the SVR performance derived from features of a particular connection length with the SVR performance derived from randomly selected features to determine whether connection distance underlies age prediction with RSFC. Randomly selected feature sets were specifically matched to have the same number of features as the 10 separate distance windows (3471 functional connections). Overall, 25 randomly selected feature sets were generated. Using 10-fold CV, a multivariate model describing the relationship between age and the RSFC in these randomly selected connections was determined and the left out participants were then tested on this SVR-derived model.

Functional systems. The brain is organized into functional systems (e.g., visual, default-mode, dorsal attention, frontoparietal) that can be revealed with RSFC at the group (Power et al. 2011; Yeo et al. 2011) and individual (Laumann et al. 2015; Gordon, Laumann, Glimore, et al. 2017) levels. Previously, we and others have shown that SVM classification accuracy for distinguishing children with developmental disorders (e.g, Tourette syndrome (Greene, Church, et al. 2016), Autism Spectrum Disorder (Uddin et al. 2013)) from healthy controls varied by the functional system(s) used for SVM training. To compare how functional connections from different functional systems contribute to age prediction, we divided the resting-state correlations according to the thirteen functional systems defined in Power et al. 2011, including control systems (frontoparietal, cingulo-opercular, salience, ventral attention, dorsal attention), processing systems (somatomotor-body, somatomotor-mouth, visual, auditory, memory), the default-mode system, a subcortical system, and a cerebellar system depicted in Figure 1A (Power et al. 2011). For each system-level comparison, functional connections within the system and functional connections between that system and the other systems were included. Using 10-fold CV, a multivariate model describing the relationship between age and the RSFC in connections associated with a particular functional system was determined and the left out participants were then tested on this SVR-derived model.

Matched feature set and null model comparison. Performance with each system-selective model was then compared with SVR performance derived from randomly selected features matched to have the same number of features as each functional system (see Prediction Across Feature Numbers). Using 10-fold CV, a multivariate model describing the relationship between age and the RSFC in these randomly selected connections was determined and the left out participants were then tested on this SVR-derived model.

RSFC strength. While strong positive resting-state correlations have dominated most RSFC studies, strong negative functional connections, as well as weakly positive or negative functional connections, might also change in development and be useful for age prediction. Previously, Bassett et al. (2012) observed that SVM classification accuracy for distinguishing patients with schizophrenia from healthy controls differed when separately including features with strong positive and weakly positive RSFC; weakly positive functional connections were more predictive than strongly positive or moderately positive functional connections. To separately consider how functional connections of different RSFC strength contribute to age prediction, we divided resting-state correlations within each individual into 10 separate windows based on the strength of each connection (3471 functional connections per window). Specifically, features were sorted by RSFC strength within each individual and a window of 10% of these functional connections were selected (note: this is distinct from features ranked according strength of correlation between RSFC and age; see Univariate Feature Ranking and Selection in Training Set). For example, connections with the strongest positive RSFC per individual, regardless of the actual correlation value, were included in the top 10% strong positive window (i.e., 1 if present or 0 if not present). Importantly, the actual functional connections selected for each window depended upon each individual's correlation matrix and varied across individuals. The lack of correspondence in the location of these functional connections across individuals is the information used for age prediction. For example, a functional connection that is in the top 10% strong positive window for one subject but not another would provide useful information for age prediction, while a functional connection that is in the top 10% strong positive window across all participants would not. Using 10-fold CV, a multivariate model describing the relationship between age and the functional connections of a particular correlation RSFC strength (e.g., strong positive, weak, strong negative) was determined and the left out participants were then tested on this SVR-derived model.

Matched feature set and null model comparison. The performance of these correlation-magnitude models was compared with a null model of features matched in number but randomly sampled from the distribution of resting-state correlations. Specifically, features were ranked by correlation magnitude within each individual, as before, but a random set of 10% of these ranks were selected. Importantly, this random set of ranks was consistent across subjects. Overall, 25 randomly selected feature sets were generated. Using 10-fold CV, a multivariate model describing the relationship between age and the location of these randomly selected connections of was determined and the left out participants were then tested on this SVR-derived model.

Intercorrelation Among Features in Feature Sets
The usefulness of a feature set can be reduced if there is a large amount of intercorrelation among features (Guyon and Elisseeff 2003). Correlated features are likely to provide redundant information for multivariate machine learning, increasing the likelihood of suboptimal predictive performance. Thus, we tested whether the feature sets described above (i.e., data-driven and hypothesis-driven feature selection) were more intercorrelated than feature sets with randomly selected features. For each feature set, we calculated the correlation between the RSFC values in each pair of functional connections across all individuals. Using a matched number of randomly selected functional connections, we calculated the intercorrelation in those feature sets as well. Because differences in both the mean (Fig. S6B) and shape (Fig. S6D) of this intercorrelation distribution indicate an increased number of intercorrelated features (see Supplemental Material H), we computed the proportion of feature pairs with an intercorrelation greater than $r = 0.2$ (2 standard deviations greater the mean of in the intercorrelation of features in the full correlation matrix) in order to quantify the amount of redundancy in each feature set. To further explore the impact of redundancy among functional connections on age prediction, we employed the Fast Correlation-Based Filter (Yu and Liu 2004) that aims to reduce the number of collinear features. With this approach, features are iteratively removed from a feature set if correlated with other, stronger (more correlated with age) features above a predetermined threshold. More details are provided in Supplemental Material H.

Results

After Motion Denoising, Individual Head Motion Cannot be Predicted From RSFC, While Age Can

First, we aimed to determine whether there was information available to predict measurement of head movement (mean FD) in RSFC before and after motion denoising. Motion-related artifact was minimized with GSR and conservative frame censoring (Power et al. 2014; Ciric et al. 2017). SVR using a 10-fold CV procedure was used to test the multivariate relationship between RSFC and head motion as well as the multivariate relationship between RSFC and age. As is shown in Figure 2A,B, age was successfully and robustly predicted at the individual level in data with and without motion denoising. In contrast, individual measurements of head motion could not be successfully predicted after reducing motion-related artifact. The amount of variance in RSFC explained by age or head motion can be quantified by comparing the true labels and SVR-predicted labels for each participant. Using the resting-state correlations between the full set of 264 ROIs, 57% of the variance in individual RSFC was explained by age with motion denoising ($r = 0.75$, $P < 0.001$, $R^2 = 0.57$), while only 44% was explained by age without motion denoising ($r = 0.66$, $P < 0.001$, $R^2 = 0.44$). Alternatively, 50% of the variance in RSFC was explained by individual head movement before reducing motion-related artifact ($r = 0.71$, $P < 0.001$, $R^2 = 0.50$), while only 4% was explained by head motion after GSR and conservative frame censoring ($r = 0.2$, $P = 0.03$, $R^2 = 0.04$).

Additionally, after sufficient motion denoising, SVR-predicted ages were less correlated with an individual's head movement. If individual head motion and age cannot be disentangled, predicted ages may still be confounded by motion-related variance in RSFC. Before motion denoising, the ages predicted from the multivariate patterns in RSFC were negatively correlated with mean FD ($r = -0.44$, $P < 0.001$, $R^2 = 0.20$). After reducing motion-related artifact, the relationship between RSFC-predicted ages and individual mean FD was markedly reduced ($r = -0.32$, $P < 0.001$, $R^2 = 0.10$).

To determine the impact of different components of motion denoising on the multivariate effects of head motion on RSFC, we tested how well patterns of partially denoised RSFC (GSR alone, frame censoring alone) could be used to predict measurements of individual head movement. Of the steps that best remove systematic differences in RSFC, GSR alone eliminated

most multivariate information related to an individual's head movement ($R^2 = 0.04$). Frame censoring alone also reduced multivariate effects of head motion as measured by mean FD across all data (preframe censoring mean FD, $R^2 = 0.10$). However, frame censoring alone was not sufficient to reduce the multivariate effects of residual head motion after frame censoring (postframe censoring mean FD, $R^2 = 0.20$, Supplemental Material C). Figure 2C shows that, while age information is

preserved, information about individual-level head movement is drastically reduced after GSR or after frame censoring.

In order to further interrogate the robustness of multivariate information related to age and head motion in RSFC, we tested the multivariate prediction of age and mean FD across many different feature sets. SVR performance for predicting age increased with the number of features (i.e., functional connections) included in training and testing as shown in Figure 2D.
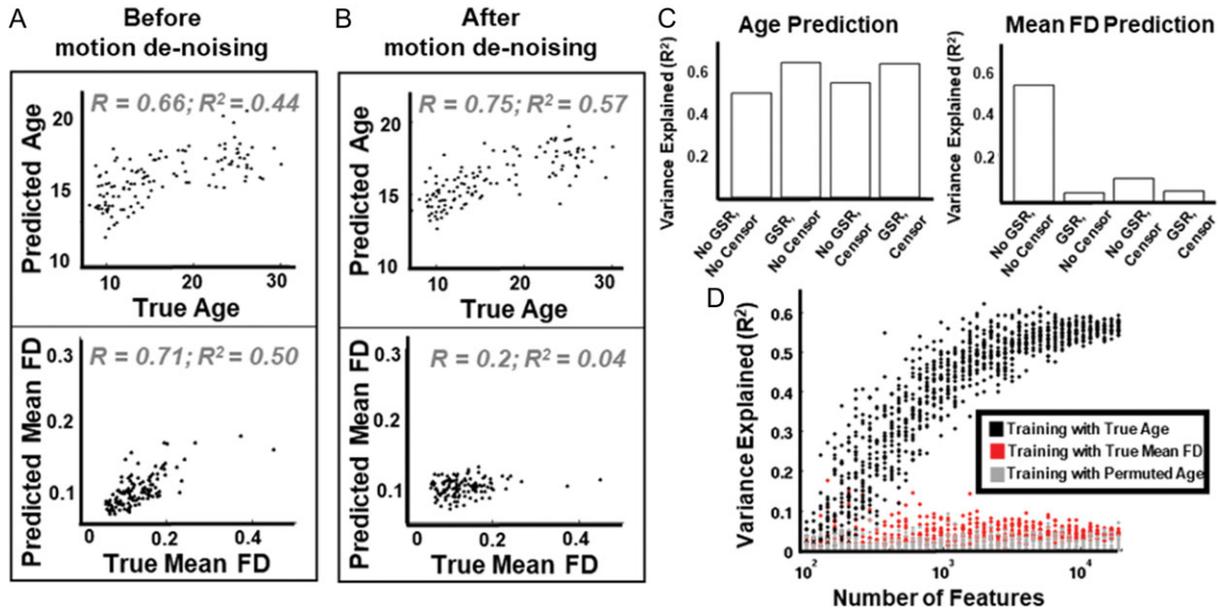
Figure 2. Motion denoising affects whether RSFC predicts head motion, but not age. (A) Predicted age (top) and predicted mean FD (bottom) of individuals in the testing set compared with the true chronological age and true mean FD of each individual. Predictions were generated from RSFC before motion denoising. (B) Predicted age (top) and predicted mean FD (bottom) of individuals in the testing set compared with the true chronological age and true mean FD of each individual. Predictions were generated from RSFC after motion denoising. (C) Age prediction (left) and mean FD prediction (right) with RSFC that has undergone no motion denoising, partial motion denoising, and full motion denoising. (D) Performance of SVR-derived models across feature sets with different number of features. A total of 25 feature sets were created by randomly selecting functional connections in 45 logarithmic increments.
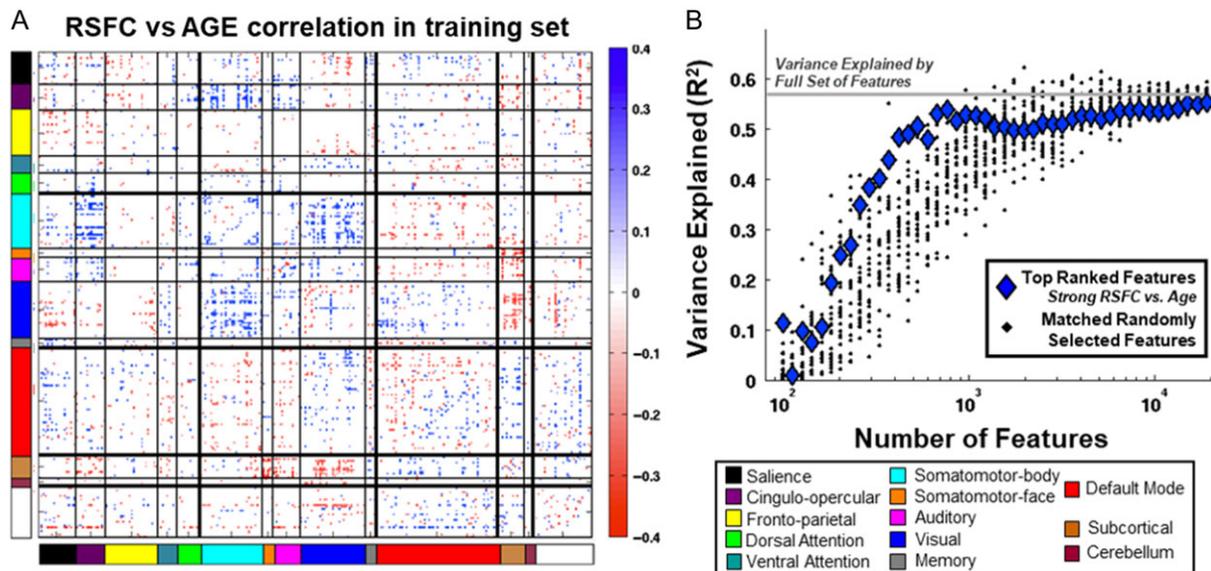
Figure 3. RSFC with strong, univariate age relationships predict age no better than randomly selected RSFC with multivariate SVR. (A) An example of the top ranked features (Consensus Features from 10%, 3471 features) across training sets. The correlation between RSFC and age was generated for these features and sorted according to functional systems. (B) Performance of SVR-derived models built with top ranked features and randomly selected features using different numbers of features. Feature sets were selected in logarithmic increments.

As an experimental control, the multivariate relationship between RSFC and permuted age labels was derived with SVR in a training set and used to predict the age of test individuals. As expected, performance of this experimental control model was poor ($r = 0.08$, $P = 0.183$, $R^2 = 0.006$). While SVR performance for predicting age far surpassed this experimental control, the performance predicting mean FD with adequately denoised RSFC did not outperform the experimental control.

Top Ranked Functional Connections Predict an Individual's Age, but not Better Than Random Functional Connections

Using data-driven feature selection, we aimed to determine a set of features that optimally predict age with SVR. Multivariate models were built with the functional connections with the strongest correlation with age within each training set (e.g., Fig. 3A: Consensus Features in Top Ranked 10%). Features with strong age relationships in the training set were able to predict the age of test individuals reasonably well, peaking at 57% of the variance explained. Figure 3B shows how the amount of developmental variance explained in the testing set depends upon the number of features included in the model. Models built from a limited set of top ranked features matched, but never predicted age better than, the model build from the full correlation matrix (i.e., 57% variance explained) even though features weakly related to age were removed. Furthermore, the SVR performance of top ranked features was not significantly better than the performance of models built from randomly selected features of the same number, as shown in Figure 3B. Some feature sets of intermediate number appear to produce marginally better age prediction than randomly selected features, suggesting that there might be a specific range of features which facilitate age prediction. However, further investigation of top ranked features with a different cross-validation protocol (training set of 90 and testing set of 32, instead of 10-fold CV) indicates the performance of top ranked features does not differ from randomly selected features across feature numbers (see Supplemental Material G). Taken together, these different validation approaches indicate that the functional connections that are most correlated with age do not uniquely or especially facilitate age prediction.

After Motion Correction, Connection Length Does not Contribute to Improved Age Prediction

Given previous suggestions of a local-to-distributed development of brain networks (Fair et al. 2009; Supekar et al. 2009; Dosenbach et al. 2010), we next aimed to compare how functional connections of different length (e.g., short-range, long-range) contribute to age prediction. Multivariate models were built with features defined by connection distance. These models were able to predict the age of a left out individual well ($R^2 = 0.49 \pm 0.04$; Fig. 4). However, SVR performance of features selected by connection length was not better than the performance of models built from a matched set of randomly selected features. Additionally, prediction was uniform across different connection distances, with neither short- nor long-range connections facilitating age prediction in comparison to mid-range connections. Age prediction in these feature sets, while comparable to age prediction in randomly selected feature sets, did not depend on the length of the functional connections used to comprise the SVR-derived model.

Different Functional Systems can Predict Age, but Poorer Than Distributed Features

We next aimed to compare how connections from different functional systems contribute to age prediction, given evidence that brain systems may develop at different rates (Gogtay et al. 2004). Multivariate models were built by selecting features from each functional system individually. These models were able to predict age to some extent (Fig. 5). However, prediction performance varied largely as a function of the number of features within each system. Notably, the SVR performance of features selected from each functional system was worse than the
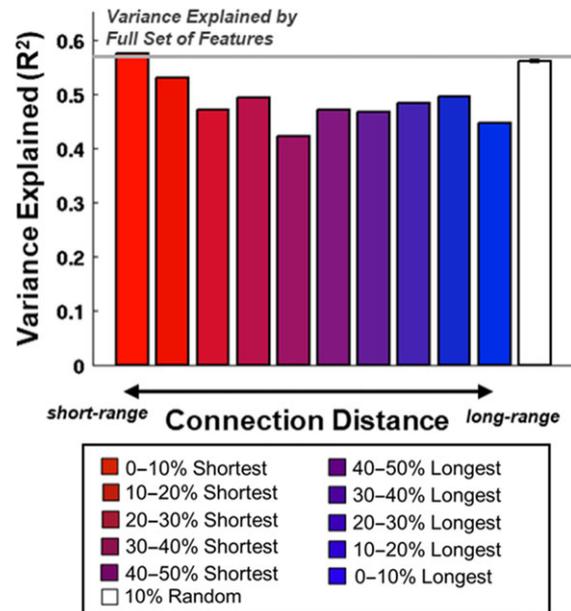
Figure 4. After motion correction, connection length does not contribute to age prediction. Performance of SVR-derived models built with features selected by connection length and features selected randomly (10%, 3471 features).
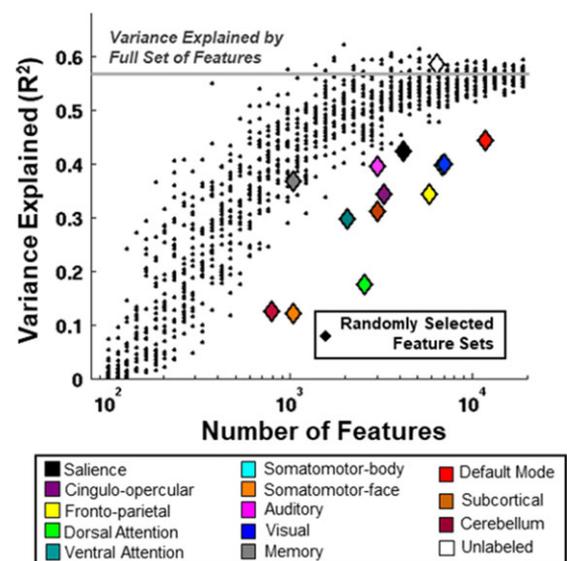
Figure 5. No single functional system predicts age better than randomly selected functional connections. Performance of SVR-derived models built with features selected from single functional systems and features selected randomly (matched by size).

performance of models built from randomly selected features that were distributed across multiple functional systems. Thus, functional connections from individual functional systems carry less information to predict age than functional connections randomly distributed across the brain and the differences in age prediction performance between different functional systems vary largely based on system size rather than system identity.

Strong Positive and Strong Negative Connections Predicts Age Better Than Weak Connections

Finally, we compared how connections from different parts of an individual's correlation distribution (i.e., strong positive, weak, strong negative) contribute to age prediction, given suggestions that even weak magnitude RSFC can improve prediction in disease states (Bassett et al. 2012). The observed location of strongly positive, weak, and strongly negative RSFC across all individuals in the developmental dataset is shown in Figure 6A–C. Strong negative RSFC was most frequently found between the DMN and other systems, and the strong positive RSFC was most frequently found within systems along the diagonal across all individuals. Weak RSFC was present in more variable locations across individuals. Multivariate models based on the location of strong positive and strong negative RSFC within an individual were able to predict age well (strong positive $R^2 = 0.54$; strong negative $R^2 = 0.47$). In contrast,
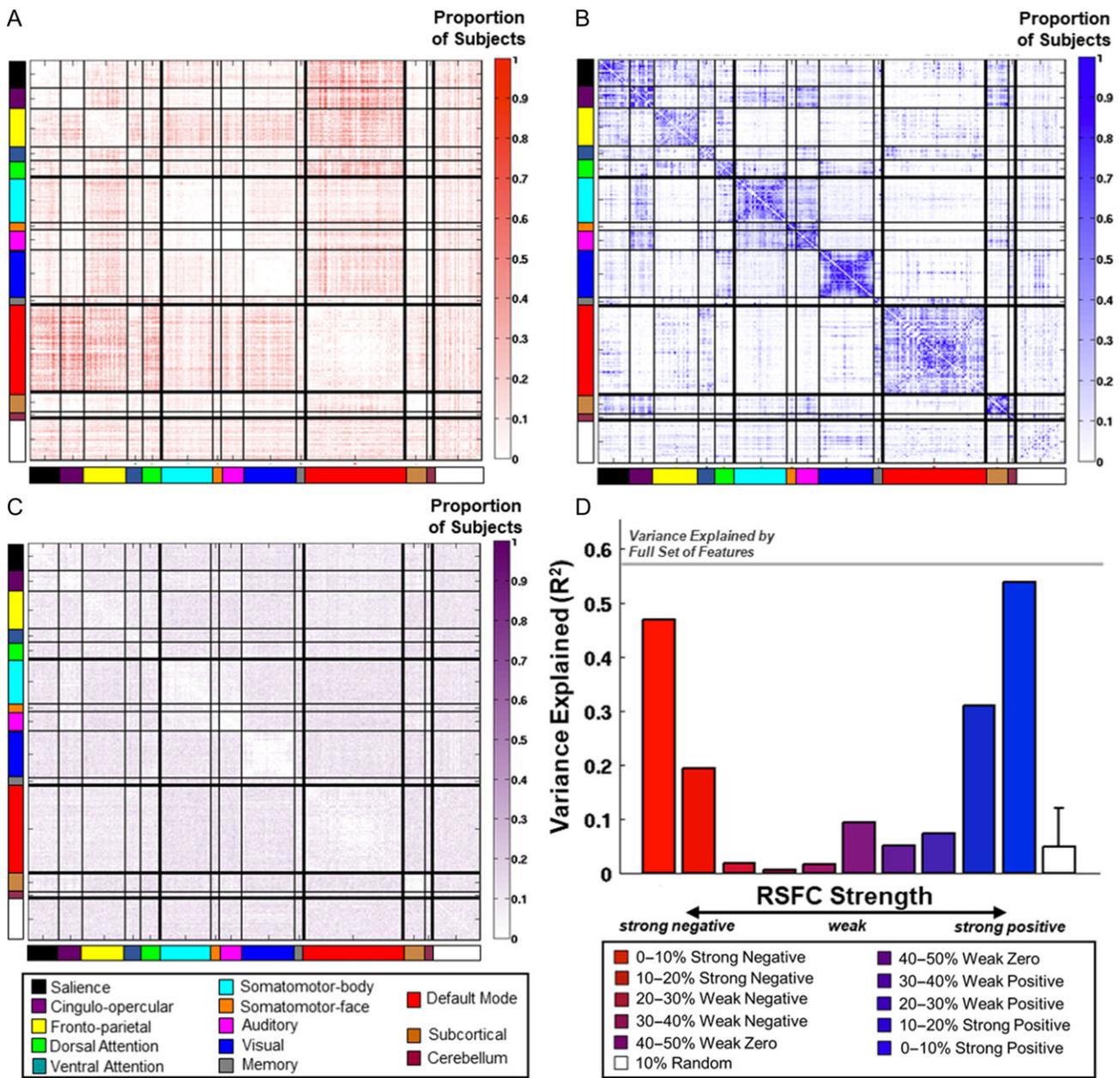
Figure 6. RSFC strength contributes to age prediction. (A) The distribution of strong negative resting-state correlations across all individuals in the developmental dataset. (B) The distribution of strong positive resting-state correlations across all individuals in the developmental dataset. (C) The distribution of weak zero resting-state correlations across all individuals in the developmental dataset. (D) Performance of SVR-derived models built with features selected by correlation strength and features selected randomly from the correlation distribution (10%, 3471 features).

multivariate models built from sets of features with weak functional connections were not able to predict age well as depicted in Figure 6D. The SVR performance of features with strong positive and strong negative RSFC was better than the performance of models built from a matched set of randomly selected functional connections.

Some Feature Sets Contain More Redundant Features Than Randomly Derived Feature Sets

Intercorrelated features may hinder multivariate age prediction because they may provide redundant information. Figure 7 compares the amount of intercorrelation among different feature sets and demonstrates that age-correlated functional connections are consistently more intercorrelated across subjects than groups of randomly selected features. Additionally, functional systems, defined in part by the consistent RSFC relationships across individuals, contain features that are more intercorrelated than matched sets of randomly selected features, as might be expected. Thus, it is possible that intercorrelations among feature sets may reduce the power of age-correlated and functional system feature sets to predict age. For further characterization of the intercorrelation in these feature sets, see Supplemental Material H.

Discussion

Motion Denoising Eliminates the Multivariate Effects of Head Motion on RSFC, While Preserving Age Information

In this work, we have shown that denoising methods to minimize motion artifact (Ciric et al., 2017)—including both GSR and frame censoring—is necessary to remove multivariate effects of head motion on RSFC. Without motion denoising, patterns of RSFC could be used to successfully predict measurements of head movement (Fig. 2A). After motion denoising, we were
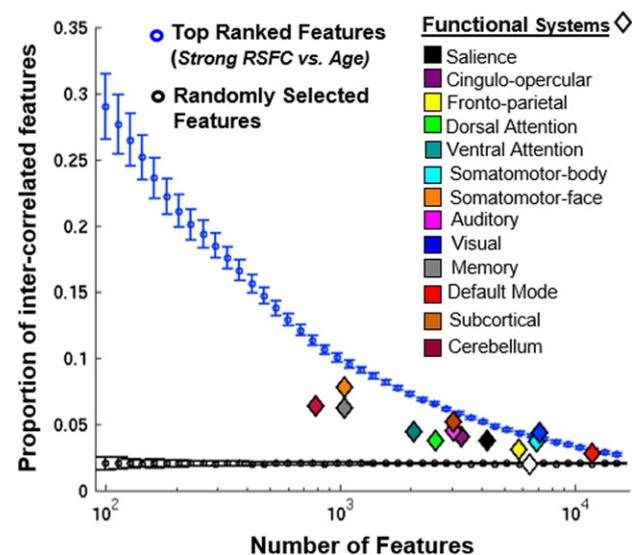
Figure 7. Proportion of intercorrelated features in the tested feature sets. Proportion of feature pairs in the tested feature set with intercorrelation greater than in the full correlation matrix (2 standard deviations greater than the mean; $r > 0.2$). The mean and 95% confidence interval of this measure of intercorrelation was generated for the top ranked features defined in each fold of 10-fold CV and for the randomly selected features across feature numbers. The intercorrelation was also generated for feature sets with functional connections from single functional systems.

unable to predict individual variability in head movement with RSFC, while still successfully predicting age (Fig. 2B). Thus, even after reducing motion-related information, RSFC carries information relevant to typical development, validating previous claims (Dosenbach et al., 2010) and supporting more recent follow-ups (Fair et al. 2013; Satterthwaite, Wolf, et al. 2013). While these previous studies have shown that age can still be predicted from RSFC after reducing motion-related artifact, our results extend such findings in a critical way by showing that there is limited lingering information about head movement as estimated with mean FD in RSFC after motion denoising.

RSFC can Predict an Individual's Age and may be a Useful Indicator of Developmental Progress

In this work, we were able to well predict an individual's age from RSFC, explaining 57% of the developmental variance across participants. Our results are comparable to previous findings of age prediction with multivariate machine learning using other measurements of the developing brain such as voxel based morphometry of T1-weighted scans ((Franke et al. 2012), R = 0.93, R^2 = 86%), volume of grey matter, white matter, and lateral ventricles ((Erus et al. 2015), R = 0.89, R^2 = 79%), and regional cortical thickness ((Khundrakpam et al. 2015), R = 0.84, R^2 = 71%). Additionally, measurements of structural connectivity, such as fractional anisotropy and diffusivity obtained with diffusion tensor imaging ((Erus et al. 2015), R = 0.89, R^2 = 79%), have also been used to successfully predict an individual's age with multivariate machine learning. Recently, task-related FC, a measurement of the transient changes in regional coherence during task performance, has been used to predict age with moderate accuracy, explaining 42% of variance related to age in a validation set (Rudolph et al. 2017). Approaches that combine information from multiple imaging modalities (T1, T2, and diffusion weighted imaging (Brown et al. 2012), R = 0.96, R^2 = 92%) have been shown to achieve the highest prediction performance. However, there is increasing evidence that head motion in the scanner systematically affects measurements of cortical thickness, grey matter volume (Reuter et al. 2015), and fractional anisotropy (Ling et al. 2012; Yendiki et al. 2014) as well as RSFC. Thus, the reported performance of multivariate age prediction with structural measurements may also be contaminated by head motion, and require additional validation.

While we (and others (Fair et al. 2013; Satterthwaite, Wolf, et al. 2013)) have shown that RSFC carries substantial information about the development of an individual (R = 0.75; R^2 = 0.57), not all characteristics of individual brain maturity are likely, nor anticipated, to be captured in resting-state correlations. For example, we know that brain size changes systematically with age (Giedd and Rapoport 2010). The distinctive utility of RSFC may lie in identifying the functional underpinnings of atypically developing individuals. RSFC, a measurement of the statistical history of co-activation across an individual's lifespan (Fox and Raichle 2007; Dosenbach et al. 2008), may be disrupted in an abnormal developmental trajectory. Because RSFC is more closely related to function than measures of brain structure, differences in RSFC might be a particularly useful indicator of dysfunction in child brain development.

After Reducing Motion-Related Artifact, Age Prediction With RSFC Does not Support the Local-to-Distributed Hypothesis of the Development of RSFC

Earlier studies of the development of RSFC organization suggested that as an individual matures, resting-state correlations shift from local, short-range connections to distributed, long-range

connections. This evidence was appealing because it agreed with neurobiological evidence of the continued myelination of long-range pathways into adolescence and adulthood (Barnea-Goraly et al. 2005). However, motion artifacts also amplify short-range RSFC and reduce long-range RSFC. While earlier attempts at age prediction with RSFC supported the local-to-distributed developmental hypothesis (Fair et al. 2009; Supekar et al. 2009; Dosenbach et al. 2010), we did not find evidence for distance-dependence in predicting age after reducing motion-related artifact. Short-range and long-range connections predicted age similarly to mid-range connections and randomly selected functional connections (Fig. 4). Other evidence based on network organization of RSFC also contradicts the local-to-distributed development of RSFC after correcting for individual head motion (Fair et al. 2013; Marek et al. 2015).

Age is Best Predicted by Strong Positive and Strong Negative RSFC Within an Individual

Because the location of strong positive and strong negative RSFC is conserved across development (Fig. 6A,B), these resting-state correlations likely represent important information about brain functioning in individuals. In most individuals in our sample, strong positive RSFC was between ROIs within functional systems and strong negative RSFC was between functional systems involved in the engagement/disengagement from tasks (e.g., DMN, FP, CO) (Fox et al. 2005). Importantly, despite the fact that these connections appear highly conserved across individuals, individual differences in the location of strong RSFC predict age well (R^2 = 0.54 and 0.47) and better than weak/moderate RSFC or randomly selected connections. While the location of weak and moderate RSFC varies more across individuals than strong RSFC, intersubject variance appears to show a negligible relationship with age (average R^2 = 0.043), and may reflect the noisy nature of these functional connections. The utility of strong-positive and strong-negative functional connections for age prediction might support previous contentions of network segregation in development (Fair et al. 2007; Satterthwaite, Wolf, et al. 2013). Strong within-network and between-network connections may be modified over the course of development in order to refine functional network organization, yet further research is necessary to directly test such claims.

Using similar approaches, others have argued that the weak resting-state correlations contain information relevant for prediction of other characteristics of an individual, such as I.Q. and psychiatric diagnosis (Bassett et al. 2012; Santarnecchi et al. 2014). We contend that the disparity in these results is related to effectively addressing motion-related artifact using volume censoring and GSR. While GSR removes the great majority of the differences in RSFC related to head motion (Power et al. 2014; Ciric et al. 2017), this procedure also shifts an individual's resting-state correlation distribution so that it becomes zero-centered and necessarily increases the number of negatively correlated functional connections (Saad et al. 2012; Power et al. 2014). Thus, previously described weak (positive or negative) connections without GSR may be equivalent to the strong negative resting-state correlations after GSR described here. In order to assess the importance of these connections in predicting an individual's age (or any characteristic), it is necessary to address motion-related artifact and to then demonstrate that the cleaned data are unable to predict that individual's head movement. As GSR eliminated most of the multivariate effects of head motion on RSFC, it is possible that weak connections without GSR could also predict measurements of head movement.

Broad Sampling of Functional Connections Yields Better Age Prediction Than Directed Sampling due to 1) the Distributed Nature of Information and 2) the Redundancy of Relevant Features

Because RSFC was able to predict an individual's age with SVR after reducing motion-related artifact, we aimed to interrogate the specific functional connections facilitating age prediction to better understand the mechanisms underlying the development of RSFC. We attempted to interrogate the features relevant to age prediction with directed, data-driven (i.e., top ranked relationships with age) and hypothesis-driven (i.e., functional systems) feature selection schemes. Unexpectedly, we found that directed sampling of functional connections yielded age prediction that was no better or, in the case of functional systems, worse than that obtained with a broad sampling of functional connections (i.e., random feature selection) (Figs 3B and 5). We have found 2 related properties of this developmental dataset that may contribute to the poorer performance of directed sampling, addressed below.

Developmental Differences in RSFC are Distributed Across Many Functional Systems

We found that information in RSFC related to age appears to be unevenly distributed in a structured way across functional systems (enriched in some blocks: e.g., many functional connections within somatomotor–visual have a strong positive correlation with age, see Fig. 3A), but resides in all functional systems. Because of the distributed nature of age-related RSFC, there may be many sets of features that are able to predict age well, even when randomly selected. Multivariate approaches are particularly well-suited to use patterns of features with variable age relationships to predict age (Jimura and Poldrack 2012). Thus, in random feature selection, by chance, relevant features across multiple functional systems are often captured, which enables robust age prediction.

Adding to the evidence that developmental differences in RSFC are distributed across many functional systems, we found that each functional system predicted age worse than randomly selected features distributed across functional systems (Fig. 5). Poorer performance of features associated with a single functional system suggests that information from multiple functional systems is necessary to achieve optimal age prediction. We did find that age prediction differed between functional systems; however, whether these differences are related to the usefulness of information from a given functional system or the number of features associated with that system remains unclear. If the mechanism by which RSFC develops is not system-dependent, then larger functional systems may be more likely to capture relevant information for age prediction by chance. Explanation-driven approaches beyond those employed in the present study may be better able to identify the specific brain systems or pieces of specific systems that change over the course of development.

While a significant portion of the extant developmental cognitive neuroscience literature has focused on the maturation of specific brain regions (e.g., the prefrontal cortex (Casey et al. 2005)) or specific functional networks (e.g., the default mode (Supekar et al. 2010)), the present results suggest that investigations of the maturation of functional neuroanatomy might be

more usefully addressed by a whole-brain or large-scale network approach. From a complex network perspective, the observation that developmental changes in functional connections are distributed across multiple systems may not be surprising. In the evolution of many complex networks, connections are modified across functional modules such that global communication is optimized and integrative hubs are created (Solé et al. 2002). It is possible that the distributed nature of developmental differences in RSFC reflects a growth mechanism that optimizes global communication rather than enhancing a single functional system. The genetics literature offers an interesting analogy with the recently proposed "omnigenic" model for the inheritance of complex traits. In this model, signal associated with complex traits is spread out across the genome (Boyle et al. 2017). Thus, one might predict that a complex characteristic of an individual, like maturity, could be supported by distributed changes in network functioning. An interesting future direction may be to determine whether more complex measures of network organization carry information useful for individual-level age prediction.

Many Functional Connections That are Relevant to Development Provide Redundant Information for Age Prediction

Although distributed across many functional systems, top ranked features (i.e., functional connections that are most strongly correlated with age) did not predict age better than randomly selected features with multivariate machine learning, as we had expected (Fig. 3B). By definition, these functional connections have, on average, stronger relationships with age than randomly selected functional connections, but were no more useful for age prediction. We believe that the usefulness of top ranked features was limited by the intercorrelated information carried by these features. Even if 2 features can each predict age well individually, there is little additional information contributed to facilitate age prediction if the pair of features are highly correlated, as they may use the same underlying information for age prediction (Guyon and Elisseeff 2003). Given that the top ranked features were much more highly intercorrelated across participants than randomly selected features (Fig. 7), this redundancy may explain why these features predicted age no better than randomly selected features. We tested this hypothesis by removing redundant features using a Fast Correlation-Based Filter (Yu and Liu 2004) and found that age prediction performance decreased more slowly when removing redundant features than when randomly removing features (Fig. S7).

One likely source of redundancy is the network organization of RSFC. By definition, functional systems identified with RSFC are composed of regions with similar patterns of connectivity. The patterns of connectivity that define functional systems are largely conserved across individuals (Power et al. 2011; Mueller et al. 2013; Wang et al. 2015; Gordon et al. 2018). The redundancy within systems may also explain why functional connections from a single system cannot predict age as well as randomly selected functional connections that sample multiple systems (Fig. 5). The redundancy of features selected from functional systems is likely not unique to age prediction and might affect prediction of other characteristics of individuals with RSFC using multivariate machine learning.

While redundancy reduces the usefulness of a feature set for age prediction, it does not reduce the relevance of these features to the development of RSFC. Feature selection methods which identify orthogonal features (e.g., Partial Least Squares Regression, Principal Component Regression) might be able to produce a set of features that is more useful for age prediction than randomly selected features, though it may be difficult to interpret the neurobiological principles underlying the importance of these features in a straightforward manner. We found that feature selection aimed at reducing collinearity (Fast Correlation-Based Filter) did not yield age prediction that was better than the full set of features (Fig. S7) indicating that removing redundant information does not improve performance. Furthermore, because of the redundancy present in this developmental dataset, there are likely many interchangeably and equally useful sets of features. While multivariate machine learning may not be the best approach for determining a single set of functional connections underlying the typical development of RSFC, we have shown that it is quite robust and powerful, predicting an individual's age well from many different subsets of functional connections.

Evaluating the Utility of Multivariate Prediction With RSFC

Many researchers use multivariate machine learning in RSFC with the intent to make accurate predictions about individuals and to interrogate the neurobiological mechanism(s) underlying a predicted characteristic. We have shown that RSFC provides a robust neurobiological measurement of an individual, sufficient to make predictions about that individual's chronological age with relatively high accuracy even, notably, after correcting for systematic differences in RSFC related to subject head motion. This observation suggests that individual age prediction with RSFC could provide useful diagnostic information about the brain maturity of individuals with developmental delay or other developmental disorders—a feat that many group-level descriptions of brain development may not be able to provide. More generally, this observation demonstrates the capacity to make predictions about an individual based on patterns of RSFC.

However, we have also shown that our ability to interrogate the specific features facilitating prediction in the hopes of understanding the neural mechanisms underlying brain development is somewhat limited. Identifying a unique set of functional connections that carry information useful for age prediction with RSFC is difficult due to the intercorrelated nature of RSFC and the distributed nature of developmental differences in RSFC, as discussed above. Thus, both data-driven and hypothesis-driven feature selection were unable to reveal functional connections that predict age better than the full set of features; removing potentially irrelevant features did not boost predictive performance. Importantly, relative to other investigations, we evaluated the performance of selected features to a null model built from a matched set of randomly selected before interpreting features as meaningful to the mechanism underlying typical development. Here, most sets of selected features (excluding strong positive and strong negative RSFC; see Fig. 6D) did not predict age better than the randomly selected null, indicating that these functional connections, while useful for prediction, are not exclusively meaningful nor indicative of a unique solution to age prediction from RSFC. Our inability to identify specific features that predict age does not mean that machine learning approaches cannot be used to identify specific features that contribute to other group differences (e.g., disease status). However, the identified features should be tested against an appropriate null model before making claims about the unique utility of a set of features for prediction and intercorrelations among features should be carefully evaluated during interpretation.

Multivariate machine learning models are built to make predictions, and can only test hypotheses about neurobiological mechanisms indirectly. Both approaches that make individual-level predictions and those that test group-level differences are important to our understanding of typical and atypical development. Multivariate prediction complemented by alternative approaches directed at more mechanistic questions (e.g., group-level studies, highly sampled individuals, within-subject longitudinal studies) will likely yield the best mechanistic understanding of typically and atypically developing individuals. Here, we demonstrate that measurements of functional neuroanatomy with RSFC are sufficiently robust to make individual-level predictions of maturity in typical development and anticipate that these characterizations may have future clinical utility in making individual-level predictions about atypical development.

Supplementary Material

Supplementary material is available at *Cerebral Cortex* online.

Funding

Notes

References

Barnea-Goraly N, Menon V, Eckert M, Tamm L, Bammer R, Karchemskiy A, Dant CC, Reiss AL. 2005. White matter development during childhood and adolescence: a cross-sectional diffusion tensor imaging study. Cereb Cortex. 15: 1848–1854.

Bassett DS, Nelson BG, Mueller BA, Camchong J, Lim KO. 2012. Altered resting state complexity in schizophrenia. Neuroimage. 59:2196–2207.

Biswal B, Zerrin Yetkin F, Haughton VM, Hyde JS. 1995. Functional connectivity in the motor cortex of resting human brain using echo-planar MRI. Magn Reson Med. 34: 537–541.

Black KJ, Koller JM, Snyder AZ, Perlmutter JS. 2004. Atlas template images for nonhuman primate neuroimaging: baboon and macaque. Methods Enzymol Imaging Biol Res Part A. 385:91–102.

Boyle EA, Li YI, Pritchard JK. 2017. An expanded view of complex traits: from polygenic to omnigenic. Cell. 169:1177–1186.

Bray SL, Chang C, Hoeft F. 2009. Applications of multivariate pattern classification analyses in developmental neuroimaging of healthy and clinical populations. Front Hum Neurosci. 3:32.

Brown TT, Kuperman JM, Chung Y, Erhart M, McCabe C, Hagler DJ Jr., Venkatraman VK, Akshoomoff N, Amaral DG, Bloss CS, et al. 2012. Neuroanatomical assessment of biological maturity. Curr Biol. 22:1693–1698.

Casanova R, Whitlow C, Wagner B, Espeland M, Maldjian J. 2012. Combining graph and machine learning methods to analyze differences in functional connectivity across sex. Open Neuroimaging J. 6:1–9.

Casey B, Galvan A, Hare TA. 2005. Changes in cerebral functional organization during cognitive development. Curr Opin Neurobiol Cogn Neurosci. 15:239–244.

Chen H, Duan X, Liu F, Lu F, Ma X, Zhang Y, Uddin LQ, Chen H. 2016. Multivariate classification of autism spectrum disorder using frequency-specific resting-state functional connectivity—a multi-center study. Prog Neuropsychopharmacol Biol Psychiatry. 64:1–9.

Ciric R, Wolf DH, Power JD, Roalf DR, Baum GL, Ruparel K, Shinohara RT, Elliott MA, Eickhoff SB, Davatzikos C, et al. 2017. Benchmarking of participant-level confound regression strategies for the control of motion artifact in studies of functional connectivity. Neuroimage. 154:174–187.

Craddock RC, Holtzheimer PE, Hu XP, Mayberg HS. 2009. Disease state prediction from resting state functional connectivity. Magn Reson Med. 62:1619–1628.

Dosenbach NUF, Fair DA, Cohen AL, Schlaggar BL, Petersen SE. 2008. A dual-networks architecture of top-down control. Trends Cogn Sci. 12:99–105.

Dosenbach NUF, Koller JM, Earl EA, Miranda-Dominguez O, Klein RL, Van AN, Snyder AZ, Nagel BJ, Nigg JT, Nguyen AL, et al. 2017. Real-time motion analytics during brain MRI improve data quality and reduce costs. Neuroimage. 161:80–93.

Dosenbach NUF, Nardos B, Cohen AL, Fair DA, Power JD, Church JA, Nelson SM, Wig GS, Vogel AC, Lessov-Schlaggar CN, et al. 2010. Prediction of individual brain maturity using fMRI. Science. 329:1358–1361.

Du W, Calhoun VD, Li H, Ma S, Eichele T, Kiehl KA, Pearlson GD, Adali T. 2012. High classification accuracy for schizophrenia with rest and task fMRI data. Front Hum Neurosci. 6:145.

Emerson RW, Adams C, Nishino T, Hazlett HC, Wolff JJ, Zwaigenbaum L, Constantino JN, Shen MD, Swanson MR, Elison JT, et al. 2017. Functional neuroimaging of high-risk 6-month-old infants predicts a diagnosis of autism at 24 months of age. Sci Transl Med. 9:eaag2882.

Erus G, Battapady H, Satterthwaite TD, Hakonarson H, Gur RE, Davatzikos C, Gur RC. 2015. Imaging patterns of brain development and their relationship to cognition. Cereb Cortex. 25:1676–1684.

Fair DA, Cohen AL, Power JD, Dosenbach NUF, Church JA, Miezin FM, Schlaggar BL, Petersen SE. 2009. Functional brain networks develop from a "local to distributed" organization. PLoS Comput Biol. 5:e1000381.

Fair DA, Dosenbach NUF, Church JA, Cohen AL, Brahmbhatt S, Miezin FM, Barch DM, Raichle ME, Petersen SE, Schlaggar BL. 2007. Development of distinct control networks through segregation and integration. Proc Natl Acad Sci. 104: 13507–13512.

Fair DA, Nigg JT, Iyer S, Bathula D, Mills KL, Dosenbach NUF, Schlaggar BL, Mennes M, Gutman D, Bangaru S, et al. 2013. Distinct neural signatures detected for ADHD subtypes after controlling for micro-movements in resting state functional connectivity MRI data. Front Syst Neurosci. 6:80.

Fan Y, Liu Y, Wu H, Hao Y, Liu H, Liu Z, Jiang T. 2011. Discriminant analysis of functional connectivity patterns on Grassmann manifold. Neuroimage. 56:2058–2067.

Fox MD, Greicius M. 2010. Clinical applications of resting state functional connectivity. Front Syst Neurosci. 4:19.

Fox MD, Raichle ME. 2007. Spontaneous fluctuations in brain activity observed with functional magnetic resonance imaging. Nat Rev Neurosci. 8:700–711.

Fox MD, Snyder AZ, Vincent JL, Corbetta M, Essen DCV, Raichle ME. 2005. The human brain is intrinsically organized into dynamic, anticorrelated functional networks. Proc Natl Acad Sci U S A. 102:9673–9678.

Fox MD, Zhang D, Snyder AZ, Raichle ME. 2009. The global signal and observed anticorrelated resting state brain networks. J Neurophysiol. 101:3270–3283.

Franke K, Luders E, May A, Wilke M, Gaser C. 2012. Brain maturation: predicting individual BrainAGE in children and adolescents using structural MRI. Neuroimage. 63:1305–1312.

Giedd JN, Rapoport JL. 2010. Structural MRI of pediatric brain development: what have we learned and where are we going? Neuron. 67:728–734.

Gogtay N, Giedd JN, Lusk L, Hayashi KM, Greenstein D, Vaituzis AC, Nugent TF, Herman DH, Clasen LS, Toga AW, et al. 2004. Dynamic mapping of human cortical development during childhood through early adulthood. Proc Natl Acad Sci U S A. 101:8174–8179.

Gordon EM, Laumann TO, Adeyemo B, Gilmore AW, Nelson SM, Dosenbach NUF, Petersen SE. 2017a. Individual-specific features of brain systems identified with resting state functional correlations. Neuroimage. 146:918–939.

Gordon EM, Laumann TO, Glimore AW, Newbold DJ, Greene DJ, Berg JJ, Ortega M, Hoyt-Drazen C, Gratton C, Sun H, et al. 2017b. Precision functional mapping of individual human brains. Neuron. 95(4):791–807.

Gratton C, Laumann TO, Nielsen AN, Greene DJ, Gordon EM, Gilmore AW, Nelson SM, Coalson RS, Snyder AZ, Schlaggar BL, et al. 2018. Functional brain networks are dominated by stable group and individual factors, not cognitive or daily variation. Neuron. 98(2):439–452.

Greene DJ, Black KJ, Schlaggar BL. 2016a. Considerations for MRI study design and implementation in pediatric and clinical populations. Dev Cogn Neurosci Flux Congress 2014. 18: 101–112.

Greene DJ, Church JA, Dosenbach NUF, Nielsen AN, Adeyemo B, Nardos B, Petersen SE, Black KJ, Schlaggar BL. 2016b. Multivariate pattern classification of pediatric Tourette syndrome using functional connectivity MRI. Dev Sci. 19: 581–598.

Greene DJ, Koller JM, Hampton JM, Wesevich V, Van AN, Nguyen AL, Hoyt CR, McIntyre L, Earl EA, Klein RL, et al. 2018. Behavioral interventions for reducing head motion during MRI scans in children. Neuroimage. 171:234–245.

Greene DJ, Laumann TO, Dubis JW, Ihnen SK, Neta M, Power JD, Pruett JR, Black KJ, Schlaggar BL. 2014. Developmental changes in the organization of functional connections between the basal ganglia and cerebral cortex. J Neurosci. 34:5842–5854.

Guyon I, Elisseeff A. 2003. An introduction to variable and feature selection. J Mach Learn Res. 3:1157–1182.

Hazlett HC, Gu H, Munsell BC, Kim SH, Styner M, Wolff JJ, Elison JT, Swanson MR, Zhu H, Botteron KN, et al, The IBIS Network. 2017. Early brain development in infants at high risk for autism spectrum disorder. Nature. 542:348–351.

Jimura K, Poldrack RA. 2012. Analyses of regional-average activation and multivoxel pattern information tell complementary stories. Neuropsychologia. 50:544–552.

Khundrakpam BS, Tohka J, Evans AC. 2015. Prediction of brain maturity based on cortical thickness at different spatial resolutions. Neuroimage. 111:350–359.

Koch W, Teipel S, Mueller S, Benninghoff J, Wagner M, Bokde ALW, Hampel H, Coates U, Reiser M, Meindl T. 2012. Diagnostic power of default mode network resting state fMRI in the detection of Alzheimer's disease. Neurobiol Aging. 33:466–478.

Laumann TO, Gordon EM, Adeyemo B, Snyder AZ, Joo SJ, Chen M-Y, Gilmore AW, McDermott KB, Nelson SM, Dosenbach NUF, et al. 2015. Functional system and areal organization of a highly sampled individual human brain. Neuron. 87: 657–670.

Liang SF, Hsieh TH, Chen PT, Wu ML, Kung CC, Lin CY, Shaw FZ 2012. Differentiation between resting-state fMRI data from ADHD and normal subjects: based on functional connectivity and machine learning. *Proceedings of 2012 International Conference on Fuzzy Theory and Its Applications (iFUZZY2012)*. Presented at the 2012 International Conference on Fuzzy Theory and Its Applications (iFUZZY2012). pp. 294–298.

Ling J, Merideth F, Caprihan A, Pena A, Teshiba T, Mayer AR. 2012. Head injury or head motion? Assessment and quantification of motion artifacts in diffusion tensor imaging studies. Hum Brain Mapp. 33:50–62.

Marek S, Hwang K, Foran W, Hallquist MN, Luna B. 2015. The contribution of network organization and integration to the development of cognitive control. PLoS Biol. 13:e1002328.

Meier TB, Desphande AS, Vergun S, Nair VA, Song J, Biswal BB, Meyerand ME, Birn RM, Prabhakaran V. 2012. Support vector machine classification and characterization of age-related reorganization of functional brain networks. Neuroimage. 60:601–613.

Mueller S, Wang D, Fox MD, Yeo BTT, Sepulcre J, Sabuncu MR, Shafee R, Lu J, Liu H. 2013. Individual variability in functional connectivity architecture of the human brain. Neuron. 77:586–595.

Nielsen JA, Zielinski BA, Fletcher PT, Alexander AL, Lange N, Bigler ED, Lainhart JE, Anderson JS. 2013. Multisite functional connectivity MRI classification of autism: ABIDE results. Front Hum Neurosci. 7:599.

Power JD, Barnes KA, Snyder AZ, Schlaggar BL, Petersen SE. 2012. Spurious but systematic correlations in functional connectivity MRI networks arise from subject motion. Neuroimage. 59:2142–2154.

Power JD, Cohen AL, Nelson SM, Wig GS, Barnes KA, Church JA, Vogel AC, Laumann TO, Miezin FM, Schlaggar BL, et al. 2011. Functional network organization of the human brain. Neuron. 72:665–678.

Power JD, Mitra A, Laumann TO, Snyder AZ, Schlaggar BL, Petersen SE. 2014. Methods to detect, characterize, and remove motion artifact in resting state fMRI. Neuroimage. 84:320–341.

Pruett JR, Kandala S, Hoertel S, Snyder AZ, Elison JT, Nishino T, Feczko E, Dosenbach NUF, Nardos B, Power JD, et al. 2015. Accurate age classification of 6 and 12 month-old infants based on resting-state functional connectivity magnetic resonance imaging data. Dev Cogn Neurosci. 12:123–133.

Reuter M, Tisdall MD, Qureshi A, Buckner RL, van der Kouwe AJW, Fischl B. 2015. Head motion during MRI acquisition reduces gray matter volume and thickness estimates. Neuroimage. 107:107–115.

Rudolph MD, Miranda-Domínguez O, Cohen AO, Breiner K, Steinberg L, Bonnie RJ, Scott ES, Taylor-Thompson K, Chein J, Fettich KC, et al. 2017. At risk of being risky: the relationship between "brain age" under emotional states and risk preference. Dev Cogn Neurosci. 24:93–106.

Saad ZS, Gotts SJ, Murphy K, Chen G, Jo HJ, Martin A, Cox RW. 2012. Trouble at rest: how correlation patterns and group differences become distorted after global signal regression. Brain Connect. 2:25–32.

Santarnecchi E, Galli G, Polizzotto NR, Rossi A, Rossi S. 2014. Efficiency of weak brain connections support general cognitive functioning. Hum Brain Mapp. 35:4566–4582.

Satterthwaite TD, Elliott MA, Gerraty RT, Ruparel K, Loughead J, Calkins ME, Eickhoff SB, Hakonarson H, Gur RC, Gur RE, et al. 2013a. An improved framework for confound regression and filtering for control of motion artifact in the preprocessing of resting-state functional connectivity data. Neuroimage. 64:240–256.

Satterthwaite TD, Wolf DH, Ruparel K, Erus G, Elliott MA, Eickhoff SB, Gennatas ED, Jackson C, Prabhakaran K, Smith A, et al. 2013b. Heterogeneous impact of motion on fundamental patterns of developmental changes in functional connectivity during youth. Neuroimage. 83:45–57.

Shulman GL, Pope DLW, Astafiev SV, McAvoy MP, Snyder AZ, Corbetta M. 2010. Right hemisphere dominance during spatial selective attention and target detection occurs outside the dorsal frontoparietal network. J Neurosci. 30:3640–3651.

Siegel JS, Mitra A, Laumann TO, Seitzman BA, Raichle M, Corbetta M, Snyder AZ. 2016. Data quality influences observed links between functional connectivity and behavior. Cereb Cortex. 27(9):4492–4502.

Solé RV, Ferrer-Cancho R, Montoya JM, Valverde S. 2002. Selection, tinkering, and emergence in complex networks. Complexity. 8:20–33.

Sundermann B, Herr D, Schwindt W, Pfleiderer B. 2014. Multivariate classification of blood oxygen level–dependent fmri data with diagnostic intention: a clinical perspective. Am J Neuroradiol. 35:848–855.

Supekar K, Musen M, Menon V. 2009. Development of large-scale functional brain networks in children. PLoS Biol. 7: e1000157.

Supekar K, Uddin LQ, Prater K, Amin H, Greicius MD, Menon V. 2010. Development of functional and structural connectivity within the default mode network in young children. Neuroimage. 52:290–301.

Uddin LQ, Supekar K, Lynch CJ, Khouzam A, Phillips J, Feinstein C, Ryali S, Menon V. 2013. Salience network-based classification and prediction of symptom severity in children with autism. JAMA Psychiatry. 70:869–879.

Van Dijk KRA, Sabuncu MR, Buckner RL. 2012. The influence of head motion on intrinsic functional connectivity MRI. Neuroimage. 59:431–438.

Vergun S, Deshpande AS, Meier TB, Song J, Tudorascu DL, Nair VA, Singh V, Biswal BB, Meyerand ME, Birn RM, et al. 2013. Characterizing functional connectivity differences in aging adults using machine learning on resting state fMRI data. Front Comput Neurosci. 7:38.

Wang D, Buckner RL, Fox MD, Holt DJ, Holmes AJ, Stoecklein S, Langs G, Pan R, Qian T, Li K, et al. 2015. Parcellating cortical functional networks in individuals. Nat Neurosci. 18: 1853–1860.

Wee C-Y, Yap P-T, Zhang D, Denny K, Browndyke JN, Potter GG, Welsh-Bohmer KA, Wang L, Shen D. 2012. Identification of MCI individuals using structural and functional connectivity networks. Neuroimage. 59:2045–2056.

Yendiki A, Koldewyn K, Kakunoori S, Kanwisher N, Fischl B. 2014. Spurious group differences due to head motion in a diffusion MRI study. Neuroimage. 88:79–90.

Yeo BTT, Krienen FM, Sepulcre J, Sabuncu MR, Lashkari D, Hollinshead M, Roffman JL, Smoller JW, Zöllei L, Polimeni JR, et al. 2011. The organization of the human cerebral cortex estimated by intrinsic functional connectivity. J Neurophysiol. 106:1125–1165.

Yu L, Liu H. 2004. Efficient feature selection via analysis of relevance and redundancy. J Mach Learn Res. 5: 1205–1224.